J Chem Technol Biotechnol 81:679–687 (2006)
DOI: 10.1002/jctb.1464

A calibration methodology and model-based systems analysis for SBRs removing nutrients under limited aeration conditions

Güçlü Insel,[1,2]* Gürkan Sin,[1] Dae Sung Lee,[1,3] Ingmar Nopens[1] and Peter A Vanrolleghem[1]

[1]BIOMATH, Ghent University, Coupure Links 653, B-9000 Ghent, Belgium
[2]Environmental Engineering Department, Istanbul Technical University, 34469 Maslak, Istanbul, Turkey
[3]School of Environmental Science and Engineering, Pohang University of Science and Technology, San 31, Hyoja-dong, Nam-gu, Pohang, Gyeongbuk 790-784, Korea

Abstract: A methodology is proposed for the model calibration of nutrient-removing laboratory-scale SBRs under limited aeration. Based on in-process measurements and influent wastewater characterization, the ASM2d model was modified by adding an organic nitrogen module incorporating a hydrolysis mechanism. After calibration, the simulation results showed that enhanced biological nutrient removal occurred during the fill period and under reduced aeration achieving so-called 'simultaneous nutrient removal'. A model-based systems analysis was performed in terms of the contributions of different processes to overall oxygen, nitrogen and phosphate utilization. In each phase, simultaneously occurring biological reactions were compared using the calibrated model. According to the calibrated model, 61% of all denitrified nitrate is denitrified during the mixing/filling phase. On the other hand, 17% of all denitrified nitrate is consumed by simultaneous nitrification–denitrification during the first aerobic period. The aerobic and anoxic P-removals were quantified as 73% and 12%, respectively.

Keywords: sequencing batch reactor; activated sludge model; calibration; simultaneous nutrient removal

NOTATION

ASM	Activated sludge model
COD	Chemical oxygen demand ($mgO_2\,L^{-1}$)
DO	Dissolved oxygen ($mgO_2\,L^{-1}$)
N_{DP}	Denitrification potential ($mgN\,L^{-1}$)
N_{OX}	Oxidized nitrogen ($mgN\,L^{-1}$)
S_{ND}	Soluble organic nitrogen ($mgN\,L^{-1}$)
S_{NH}	Ammonia nitrogen ($mgN\,L^{-1}$)
MLSS	Mixed liquor suspended solids ($mg\,L^{-1}$)
NUR	Nitrate utilization rate ($mgN\,L^{-1}\,h^{-1}$)
NPR	Nitrate production rate ($mgN\,L^{-1}\,h^{-1}$)
ORP	Oxidation and reduction potential (mV)
OUR	Oxygen uptake rate ($mgO_2\,L^{-1}$)
PAO	Phosphorus-accumulating organism
PRR	Phosphorus release rate ($mgP\,L^{-1}\,h^{-1}$)
PUR	Phosphorus utilization rate ($mgP\,L^{-1}\,h^{-1}$)
SBR	Sequencing batch reactor
SVI	Sludge volume index (mL/g)
TKN	Total Kjeldahl nitrogen
X_{ND}	Particulate organic nitrogen ($mgN\,L^{-1}$)
Y_{HNO_3}	Anoxic heterotrophic yield coefficient (gcellCOD $gCOD^{-1}$)
q_{PHA}	maximum acetate uptake rate of PAOs (gCOD gcellCOD^{-1} day^{-1})
VFA	Volatile fatty acid
Y_{PO_4}	Yield for phosphorus release (mgP $mgCOD^{-1}$)
η_{NO_3PAO}	Anoxic reduction factor for phosphate uptake of PAOs
$\rho_{hydrolysis}$	Hydrolysis rate in ASM2d model

NOMENCLATURE

PUR_Total:	Total phosphate utilization rate (mgP/L.h)
PUR_Xpao_aer:	Aerobic phosphate utilization rate for X_{PAOs} (mgP/L.h)
PUR_Xpao_anox:	Anoxic phosphate utilization rate for X_{PAOs} (mgP/L.h)
PUR_Het:	Phosphate utilization rate for ordinary heterotrophs (mgP/L.h)
OUR_Nitr:	Oxygen uptake rate due to autotrophic activity (mgO_2/L.h)
OUR_Het:	Oxygen uptake rate for ordinary heterotrophs (mgO_2/L.h)

* Correspondence to: Güçlü Insel, Environmental Engineering Department, Istanbul University, 34469 Maslak, Istanbul, Turkey
E-mail: inselhay@itu.edu.tr
Contract/grant sponsor: Fund for Scientific Research — Flanders (FWO)
Contract/grant sponsor: Ghent University Research Fund
(*Received 25 May 2005; revised version received 5 October 2005; accepted 19 October 2005*)
Published online 24 February 2006

OUR_Xpao: Oxygen uptake rate for X_{PAOs} (mgO_2/L.h)
NUR_Het: Nitrate utilization rate for ordinary heterotrophs (mgN/L.h)
NUR_Xpao: Nitrate utilization rate for X_{PAOs} (mgN/L.h)

INTRODUCTION

Sequencing batch reactors (SBRs) are mainly characterized by sequential process phases of fill, react, settle, decant and idle periods that allow considerable flexibility in their design and operation for different biological wastewater treatment alternatives.[1–3] This flexibility is provided by the unique features of SBRs: (a) influent and effluent flows are uncoupled by time sequencing; (b) clarification occurs in the same reactor; (c) biological processes take place in a cyclic or periodic manner; and (d) a portion of the treated water is replaced by untreated wastewater for each cycle, distinguishing the SBR process from other continuous flow-type activated sludge systems.[4,5]

The design of an SBR for nutrient (nitrogen) removal is mainly based on the selection of some relevant parameters (e.g. sludge age, volume exchange ratio, cycle time, SVI) as described in, for instance, the ATV guidelines,[6] in combination with stoichiometric mass balance calculations on the denitrification potential, N_{DP}, and oxidized nitrogen, N_{OX}.[5] In reality, the resulting wastewater treatment plants are mostly over-designed to sustain efficient carbon and nutrient removal under varying environmental and operating conditions. However, attention should be paid to the operating conditions, which may positively or negatively affect the overall system performance, even if the system is designed with safety margins. On the other hand, the optimization of operating parameters (e.g. aeration control) can be an asset as it can take advantage of simultaneous nitrogen removal together with enhanced biological phosphorus removal known as 'simultaneous nutrient removal'.[7]

An existing SBR plant may require optimization in terms of nutrient removal, but this often requires a better understanding and quantification of the biological processes occurring in each phase of the SBR operation. A calibrated activated sludge model is a practical tool to try numerous operating scenarios within a short evaluation time when an upgrade of the SBR is considered. In this way, the effect of changes in process configuration/control and environmental factors can be simulated.[8–11] However, obtaining a reliably calibrated model is not straightforward. On the contrary, it is a tedious task and involves many steps, which need appropriate guidance (for a thorough review of different guidelines, see Ref. 12). For example, calibration requires expert knowledge of the influent wastewater characterization and on-line/off-line measurements and a good knowledge of the operating conditions and the treatment system itself. The model-based interpretation of the system that can then be attempted not only leads to a better understanding of the biological processes but also provides a way of selecting the most appropriate operating variables such as cycle times and aeration capacity.

This paper describes a calibration methodology for the application of activated sludge models (ASMs) on SBR systems. The methodology was evaluated on a laboratory-scale SBR performing simultaneous nutrient removal under limited aeration conditions. In addition, a systems analysis was performed via the investigation of individual biological process contributions to phosphate utilization, oxygen consumption and nitrogen removal by using the calibrated model.

MATERIALS AND METHODS

SBR operation and process control

A pilot-scale SBR with a working volume of 80 L was seeded with sludge from the Ossemeersen wastewater treatment plant (Ghent, Belgium) and operated for a 2-year period. The hydraulic retention time (HRT) and solids retention time (SRT) were maintained at 12 h and 10 days, respectively. Each cycle comprised an unaerated fill phase (60 min), aeration phase (150 min), anoxic phase (60 min), aerated phase (30 min), settling phase (45 min) and draw phase (15 min). The total cycle time, C_T was set to 6 h (four cycles per day) with a volumetric exchange ratio (V_0/V_{Total}) of 0.5. The excess sludge was taken to waste from the end of the second aerobic phase of each cycle. The food to microorganism ratio (F/M) was adjusted to 0.10 gCOD $gMLSS^{-1}\,d^{-1}$. A schematic diagram of the SBR system is given in Fig. 1.

The controls of the duration/sequence of phases and on/off status of peristaltic pumps, mixer and air supply were automatically achieved by a LabView (National Instruments, Texas, USA) data acquisition and control (DAC) system. The DAC system consisted of computer, interface cards, meters, transmitters and solid-state relays. Sensors for pH, ORP (oxidation–reduction potential), DO (dissolved oxygen), temperature, weight and conductivity were installed and connected to the individual meters. The status of the reactor was displayed on the computer

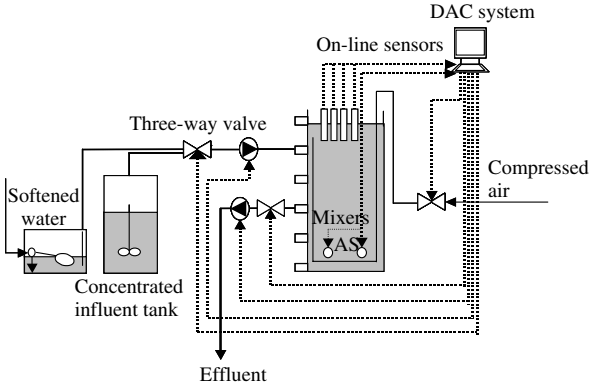

Figure 1. Schematic diagram of the SBR system.

and the time series of the electrode signals were stored in a data log-file every 2 s. The aeration was controlled by switching the aeration valve on and off. The oxygen level was kept around $2\,mgO_2\,L^{-1}$ using an on/off controller with $0.5\,mgO_2\,L^{-1}$ dead band. Measurements of orthophosphate, dissolved oxygen, ammonia and nitrate nitrogen were used in the calibration study. Daily MLSS, COD and TKN measurements were used to evaluate the long-term performance. The volumetric oxygen mass transfer coefficient, K_La, was measured to be $255\,d^{-1}$. Basically, K_La was measured at the end of the aerobic period when the oxygen uptake rate was no longer changing. K_La was calculated based on the unsteady-state mass balance by plotting oxygen concentration versus time.[13] All analytical measurements were carried out according to *Standard Methods for the Examination of Water and Wastewater*.[14]

Model-based wastewater characterization

In the modeling studies, ASM2d[15] was modified by the addition of ammonification and hydrolysis of organic nitrogen processes to deal with the observation that influent wastewater contains soluble (<0.45 μm) and particulate organic nitrogen that degraded only slowly [see the NH_4-N evolution in Fig. 4(a)]. Synthetic sewage representing pre-settled domestic wastewater[16,17] was used as SBR influent. Based on the model, the influent wastewater characterization in terms of COD fractions, nitrogen and phosphorus content is summarized in Table 1. The amount of particulate inert COD fraction (X_I) was adopted from the previous study of Boeije *et al*.[16] The rest of the COD fractions were calculated based on a mass balance over soluble and particulate COD concentrations. The soluble components were assumed to pass through a membrane filter of 0.45 μm pore size.

In the model simulations, the settling and decanting phases were characterized by a reactive point-settler model.[18] The simulations were carried out using the WEST modeling and simulation platform (Hemmis, Kortrijk, Belgium).[19]

RESULTS AND DISCUSSION

Measurement campaign results

On-line measurements were performed in the reactor (Fig. 2). The nitrification end-point, the consumption of nitrate due to denitrification and the phosphate release can be deduced from these measurements.[20] The corresponding oxygen, O_2, filtered total phosphate, PO_4-P, nitrate nitrogen, NO_3-N, and

Table 1. ASM2dN-based influent wastewater characterization (adapted from Boeije *et al*.[16])

Component	Units	Concentration	Measurement and calculation
Total COD, COD_{Tot}	$mgCOD\,L^{-1}$	411	Lab. analysis
Soluble COD, S_T	$mgCOD\,L^{-1}$	183	0.45 μm filtering
Particulate COD, X_T	$mgCOD\,L^{-1}$	228	Mass balance ($S_T - X_T$)
Inert COD, C_I	$mgCOD\,L^{-1}$	36	Mass balance ($COD_{Tot} - C_S$)
Particulate Inert COD, X_I	$mgCOD\,L^{-1}$	18	Mass balance ($C_I - S_I$)
Soluble Inert COD, S_I	$mgCOD\,L^{-1}$	18	Effluent analysis
Biodegradable COD, C_S	$mgCOD\,L^{-1}$	375	Respirometry
Fermentable COD, S_F	$mgCOD\,L^{-1}$	95	Mass balance ($S_T - S_A - S_I$)
Acetate COD, S_A	$mgCOD\,L^{-1}$	70	Gas chromatography
Slowly biodegradable COD, X_S	$mgCOD\,L^{-1}$	210	Mass balance ($C_S - S_A - S_F$)
Total Phosphate (S_{PO_4}-P)	$mgP\,L^{-1}$	11	Lab. analysis
Total Kjeldahl nitrogen, TKN	$mgN\,L^{-1}$	63	Lab. analysis
Ammonium nitrogen, NH_4-N	$mgN\,L^{-1}$	3	Lab. analysis
Soluble biodegradable nitrogen, S_{ND}	$mgN\,L^{-1}$	10	0.45 μm filtering
Particulate biodegradable nitrogen, X_{ND}	$mgN\,L^{-1}$	50	Mass balance

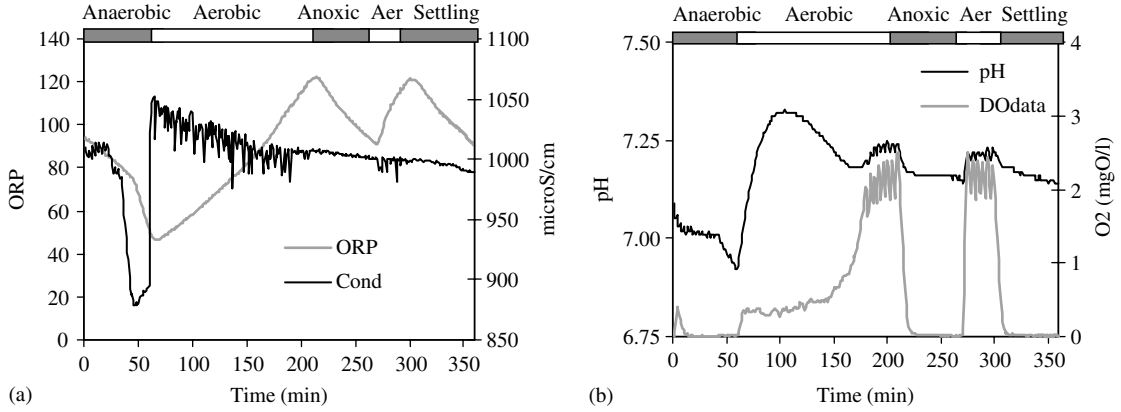

Figure 2. On-line measurements of (a) ORP and conductivity and (b) dissolved oxygen and pH.

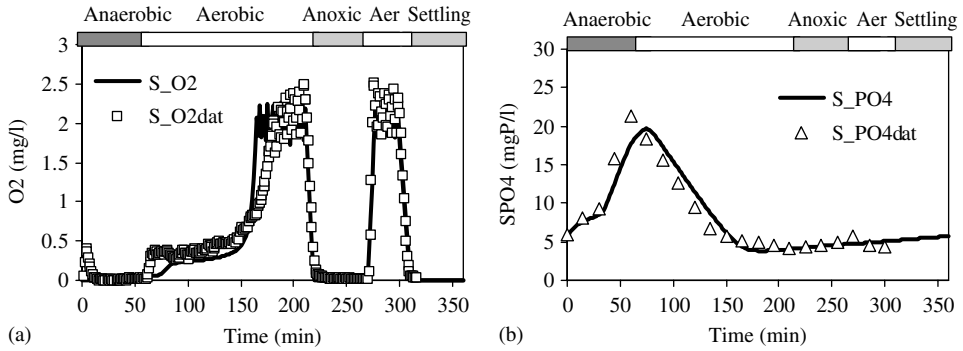

Figure 3. Measurements (symbols) and simulations (lines) of (a) dissolved oxygen and (b) phosphate.

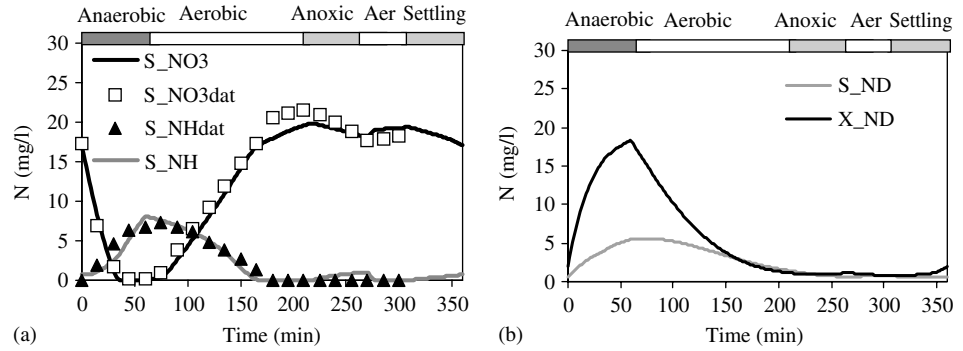

Figure 4. Measurements (symbols) and simulation (lines) of (a) NH_4/NO_3-nitrogen, and (b) soluble/particulate nitrogen.

ammonia nitrogen, NH_4-N, measurements are presented in Figs 3 and 4. The transient build-up of nitrite nitrogen was found to be negligible. This indicates that the ammonia nitrogen (NH_4-N) was fully oxidized to nitrate nitrogen (NO_3-N). At the beginning of the fill period, a small increase in oxygen concentration occurred because of an inherent oxygen transfer during the feeding and mixing. The mixed liquor temperature was measured to be around 16 °C during the SBR operation and measurement campaign. The gradual pH decrease in the anaerobic period is caused by several factors: physical (filling of acidic concentrated influent), chemical (buffers, e.g. VFAs, phosphate, bicarbonate) and biological processes (phosphate release, denitrification, etc.). As soon as the anaerobic phase starts, the above-mentioned processes take place simultaneously. The net effect of these processes is apparently a slow decrease in the pH of the medium. Towards the end of the anaerobic phase, the denitrification is completed (as can be seen in Fig. 4) and a sharp pH decrease is observed, presumably due to the phosphate release and fermentation processes which are dominant at this time instant.

During the first aerated period, the oxygen concentration is fairly low (around $0.3\,mg\,L^{-1}$) as a result of the high oxygen consumption by biomass for readily biodegradable COD degradation with fixed aeration intensity. The effect of CO_2 stripping on the pH profile seems to be higher than that of nitrification up to the middle of the aerated phase (Fig. 2). The oxygen concentration increased up to the controlled band of $2 \pm 0.5\,mgO_2\,L^{-1}$ at the end of the first aerobic phase. In the following phases, it decreased to zero since the aeration was switched off [Fig. 2(b)].

The phosphate concentration increased during the fill phase because of P-release (VFA uptake) and filling. Figure 3(b) shows that the rate of phosphorus release increased as soon as the nitrate was completely consumed. The remaining VFA was consumed with P-release.[21,22] At the end of the first phase, after a steep decline, a gradual increase in the conductivity measurements can be observed after the NO_3 consumption is completed. This could possibly be attributed to phosphorus release, which liberates ions into the bulk.[23] In the aerobic phase, the phosphate is taken up again. There is a slight increase in the phosphate concentration during the second anoxic period, probably because of endogenous P-release and COD turnover from the endogenous biomass. Complete nitrate utilization is directly correlated with a sudden change in ORP slope, so called 'nitrate knee'.[20] As shown in Fig. 2(a), the nitrate knee can be seen around 75 mV when the nitrate nitrogen (NO_3-N) is completely consumed from the bulk in the middle of anaerobic/filling phase. Then, the ORP suddenly drops to 45 mV within 15 min in parallel with the P-release at the end of the anaerobic phase [see Fig. 3(b)].

The NH_4-N and NO_3-N profiles during the first aerobic phase are interesting in terms of their order of magnitude at the end of the aerobic phase [Fig. 4(a)]. The NO_3-N generation is much higher than the observed NH_4-N consumption. This observation reveals that organic nitrogen is transformed into NH_4-N and nitrified to NO_3-N directly and that, in

fact, only a net NH_4-N conversion rate is measured. Indeed, after the complete oxidation of NH_4-N, the NO_3-N build-up continues at a lower rate until the end of the first aerobic period. Hence the degradation of organic nitrogen becomes the rate-limiting step and must be incorporated in the model in such a way that it is controlled by the hydrolysis mechanism. In the second aerobic period, NO_3-N increased from 17 to 20 mgN L^{-1}. The organic nitrogen in the effluent water was found to be around 1.0 mgN L^{-1}, which is also in agreement with the simulation result [Fig. 4(b)].

It should be stressed that the total phosphate mass balance resulted in a 98% recovery, confirming the exact total sludge age of the system. Within the observation period covering the calibration study, consistent long-term MLSS and effluent data, together with the on-line measurements, show that the system, under constant conditions, is at the steady state.

Modification of activated sludge model

The activated sludge model used was built on the basis of ASM1 and ASM2d.[15,24] According to the influent wastewater characterization and the observed nitrogen dynamics in the phases, it was decided to modify ASM2d by adding the nitrogen transformations included in ASM1. The underlying reason is as follows: the total nitrogen (TN) of the influent is 63 mgN L^{-1}, of which 3 mgN L^{-1} is NH_4-N (see Table 1). At the end of the filling phase, therefore, the expected TN concentration is about 31.5 mgN L^{-1} (the dilution introduced by the influent filling is half and the release of organic nitrogen from the decay process is assumed to be negligible for a 1 h duration), which is also confirmed by the measurement. The NH_4-N at the end of the anaerobic phase was measured as 8.21 mgN L^{-1} (see Fig. 4).

This means that only about 7 mgN L^{-1} of TN was hydrolyzed into NH_4-N while the rest remained in the form of organic nitrogen (soluble and particulate). Hence an approach similar to ASM1 was used, i.e. the particulate nitrogen is first hydrolyzed to soluble organic nitrogen, S_{ND}, and then ammonified to NH_4-N by heterotrophic biomass. The kinetics of the ammonification process were adopted from the ASM1 model.[24] In ASM1, the reaction rate for the ammonification process is expressed as first-order kinetics to describe the transformation of soluble organic nitrogen to ammonia (NH_4-N). Compared with the rate of organic particulate organic nitrogen hydrolysis, the ammonification rate is much higher and it was modeled as $k_a S_{ND} X_H$. The ammonification rate constant, k_a, was set to its default value of 0.06 d^{-1}. The hydrolysis of organic nitrogen was coupled to organic carbon hydrolysis. In Table 2, the modified part of the ASM2d is given in Peterson matrix format.

The hydrolysis kinetics under anaerobic and anoxic conditions were adapted with correction factors. The kinetics and stoichiometry for autotrophs, heterotrophs and phosphorus accumulating microorganisms were taken from the ASM2d model, except for the anoxic heterotrophic yield, Y_{HNO_3}, which is suggested to be different from the aerobic yield.[25,26] The default values of the parameters were taken as the starting point. The phosphorus components (soluble and particulate) were taken as a fraction of the influent COD fractions and model components. The conservation of the components was calculated according to Gujer and Larsen.[27]

Calibration methodology

A stepwise calibration methodology was developed based on long-term simulations in each iteration.

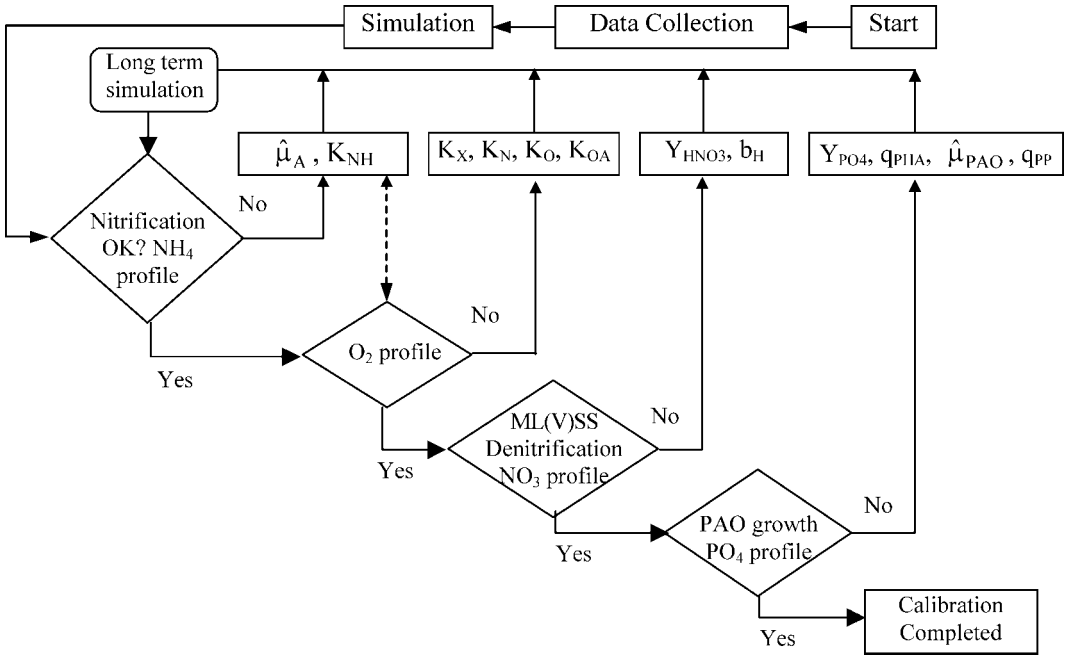

Figure 5. Calibration methodology for the ASM2dN model.

Table 2. Modified part of the ASM2d as a nitrogen module

Process	S_{NH}	S_{ND}	X_{ND}	Process rate
Hydrolysis of entrapped nitrogen		1	−1	$\rho_{hydrolysis} \frac{X_{ND}}{X_S}$
Ammonification	1	−1		$k_a S_{ND} X_H$

As illustrated in Fig. 5, a calibration methodology based on expert knowledge was constructed by introducing four iterative steps sequentially evaluating the NH_4-N, O_2, NO_3-N and PO_4-P profiles. For each iteration, a 30-day simulation was carried out to ensure that the state variables gave the same trend in each cycle ('steady state'). The starting point was to obtain the proper activity of the autotrophs to generate NO_3-N. In the first long-term simulation with the default parameter values, the autotrophs were washed out from the system. As a result, the nitrogen half saturation coefficient for autotrophs, K_{NH}, was decreased because of the low ammonia concentration in the aerobic phase. Next, the maximum growth rate for autotrophs, $\hat{\mu}_A$, had to be increased in order to sustain autotrophic growth. Later, the oxygen half saturation constants for autotrophs, K_{OA}, and heterotrophs, K_O, were changed to promote heterotrophic growth. In addition, the half saturation constant for hydrolysis, K_X, was included in the calibration to obtain a better fitting of the O_2 profile [Fig. 3(a)]. It should be noted that each iteration step involved repeating the preceeding steps to maintain good NH_4-N, O_2, NO_3-N and PO_4-P predictions.

In the third step, the anoxic yield, Y_{HNO_3}, was adjusted (0.58 gcellCOD $gCOD^{-1}$) in order to increase the denitrification potential and fit the measured nitrate concentrations. In the literature, the anoxic yield was also reported to be lower than the aerobic yield coefficient.[25,26]

Fitting the MLSS component could be added to Fig. 5, but no additional calibration effort was needed for this case. The MLSS was measured and simulated to be around 2000 mg L^{-1} when the volume reached its maximum (V_{Total}). The simulated soluble nitrogen, S_{ND}, and particulate nitrogen, X_{ND}, profiles are illustrated in Fig. 4(b). Finally, the fourth step deals with the calibration of the kinetic constants for the PAOs. The maximum acetate uptake rate of the PAOs, q_{PHA}, had to be increased in order to have them compete successfully with ordinary heterotrophs during the fill phase in the presence of NO_3-N. The reason is that the high NO_3-N concentrations during the first 30 min of the fill phase caused a high denitrification rate, which consumed VFA before the true anaerobic period began.

In order to determine the anoxic to aerobic P uptake ratio (η_{NO_3PAO}) anaerobic–aerobic and anaerobic–anoxic phosphate uptake tests were carried out according to Ref. 28 (results not shown). In the ASM2d model,[15] the X_{PAO} anoxic P-storage rate is reduced by the η_{NO_3PAO} factor. With the current SBR operation strategy, it was difficult to estimate this factor owing to the complex structure of the model. To obtain a value, a mixed liquor sample was taken from the reactor, washed and subjected to anaerobic conditions by injecting acetate, then it was separated into two equal portions. After obtaining time-dependent phosphate profiles, the ratio of the anoxic phosphate uptake rate to the aerobic phosphate uptake rate provided the η_{NO_3PAO} factor. The η_{NO_3PAO} value was found to be around 0.6, which agrees with the proposed default value in ASM2d. The yield for phosphate release, Y_{PO_4}, had to be decreased to fit the fill-phase PO_4-P profile. As stated in the ASM2d model, the storage compound, X_{PHA} is consumed by two simultaneous processes, which are phosphate uptake and the growth of PAOs. During calibration, X_{PAOs} was increased by adjusting the maximum growth rate of PAOs, $\hat{\mu}_{PAO}$, to a higher value of 1.5 day^{-1}. Meanwhile, to achieve a steeper slope and also to reach a constant PO_4 concentration at the end of the aerobic phase, the maximum phosphate uptake rate, q_{PP}, was increased [Fig. 4(b)]. The calibration task was terminated when the simulated profiles were closest to all measured data (see Figs 2–4). The values of the

Table 3. Summary of the calibrated ASM2dN parameters

Parameter	Units	Default	Calibrated
Heterotrophs, X_H			
Anoxic heterotrophic yield, Y_{HNO_3}	gcellCOD $gCOD^{-1}$	0.63	0.58
Endogenous decay rate for heterotrophs, b_H	d^{-1}	0.4	0.45
Half saturation constant for hydrolysis, K_X	gCOD $gcellCOD^{-1}$	0.1	0.045
Saturation/Inhibition coefficient for O_2, K_O	$mgO_2\,L^{-1}$	0.2	0.06
Phosphorus-accumulating organisms, X_{PAO}			
Half saturation constant for ammonia (heterotrophs), K_N	$mgN\,L^{-1}$	0.05	0.01
Yield coefficient for phosphate release, Y_{PO_4}	gP $gCOD^{-1}$	0.4	0.38
Rate constant for storage of PHA, q_{PHA}	gCOD $gPP^{-1}\,d^{-1}$	3.0	6.0
Maximum phosphorus storage rate, q_{PP}	gP $gcellCOD^{-1}\,d^{-1}$	1.5	1.3
Maximum growth rate for PAOs, $\hat{\mu}_{PAO}$	d^{-1}	1.0	1.8
Autotrophs, X_A			
Maximum growth rate for autotrophs, $\hat{\mu}_A$	d^{-1}	1.0	1.5
Saturation coefficient for O_2 (autotrophs), K_{OA}	$mgO_2\,L^{-1}$	0.5	0.07
Half saturation constant for ammonia (autotrophs), K_{NH}	$mgN\,L^{-1}$	1.0	0.2

calibrated parameters together with their default values are given in Table 3. This calibrated model was successfully used to increase the removal efficiency of the SBR under study.[10] In this way, the credibility/validity of the calibrated model could be tested together with the calibration methodology developed here.

Model-based systems analysis

Activated sludge systems, e.g. SBRs, are characterized by rather dynamic and complex behaviors in which a myriad of processes (biological, physical and chemical) interact with one another. Dynamic modeling makes it possible to perform steady-state calculations of the contributions of each process in the system. This helps in understanding the effect of each process on the system performance. For instance, the dissolved oxygen level is a result of complex process interactions between aeration intensity and biological activities, e.g. endogenous respiration and autotrophic respiration, that can be studied by dynamic simulations.

Using the calibrated model, the trajectories of the process rates were drawn to visualize the contribution of each process to the overall SBR behavior. It is obvious from Fig. 6(a) that the P-release rate (PRR) after the middle of the fill phase was 2.5 times higher ($21\,\mathrm{mgP\,L^{-1}\,h^{-1}}$) than that at the beginning of the phase ($7.5\,\mathrm{mgP\,L^{-1}\,h^{-1}}$) because of the disappearance of NO_3-N. According to the model simulations, the availability of NO_3-N during the anaerobic phase leads to a decreased PRR. The reason is that the anoxic growth of heterotrophic biomass (X_H) and the storage process by X_{PAO}s compete for VFA. The ordinary heterotrophs (X_H) play a dominant role in nitrate removal via denitrification consuming VFA (S_A) and fermentable substrate (S_F).

The PRR is maintained until the external carbon source is completely consumed after around 100 min and the oxygen concentration increased. The nitrate production rate (NPR) immediately increased when aeration was turned on. The rate dropped from 13 to around $5\,\mathrm{mgN\,L^{-1}\,h^{-1}}$ when it became hydrolysis limited (at 160 min).

The simulation of the total phosphate utilization rate (PUR) revealed that the largest contribution can be attributed to the aerobic phosphate uptake by the PAOs (73% of the total P uptake) initially exhibiting an uptake rate of $11\,\mathrm{mgP\,L^{-1}\,h^{-1}}$ [Fig. 6(b)]. As can be observed from Figs 6(b) and 7, P-release, anoxic P-uptake and VFA storage occurred simultaneously. It is important to mention that 19% of the removed P was taken up by the PAOs anoxically during the fill phase (12%).

In the aerobic phase, another 73% of P is stored [Fig. 8(a)]. The anoxic P-uptake rate at the start of the aerobic phase was simulated to be around $1.4\,\mathrm{mgP\,L^{-1}\,h^{-1}}$. The P-uptake via heterotrophic growth only covers 8% of the overall P-removal (growth of nitrifiers is neglected).

According to the simulation results, the distribution of denitrified nitrogen over each of the phases can be summarized as follows: (a) 61% of total denitrification occurred in the first phase (fill phase); (b) 17% was denitrified under aerobic conditions due to simultaneous nitrification–denitrification;[29,30] (c) only 10% denitrification was achieved in the dedicated second anoxic period; and (d) 10% denitrification in

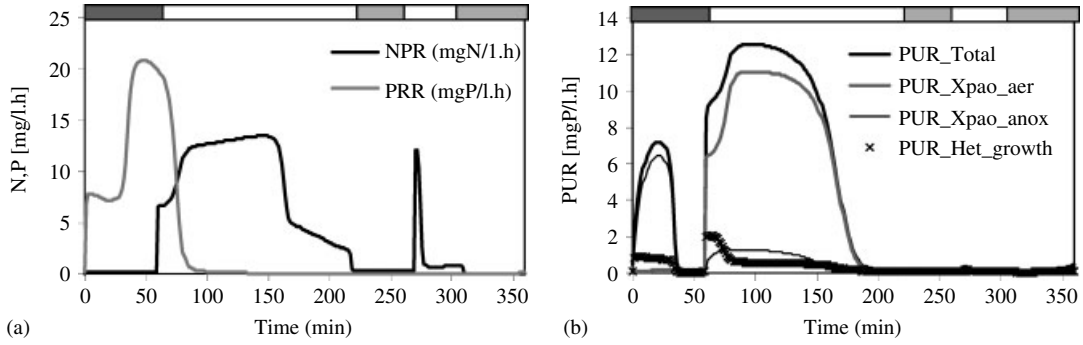

Figure 6. Simulations results for (a) Nitrate production rate, P-release rate and (b) contributions of phosphate utilization rates.

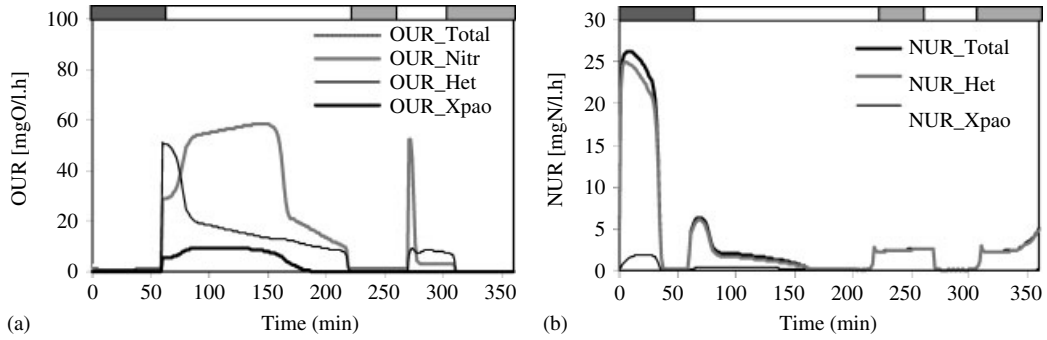

Figure 7. Simulation results for (a) OUR and (b) NUR contributions in a SBR cycle.

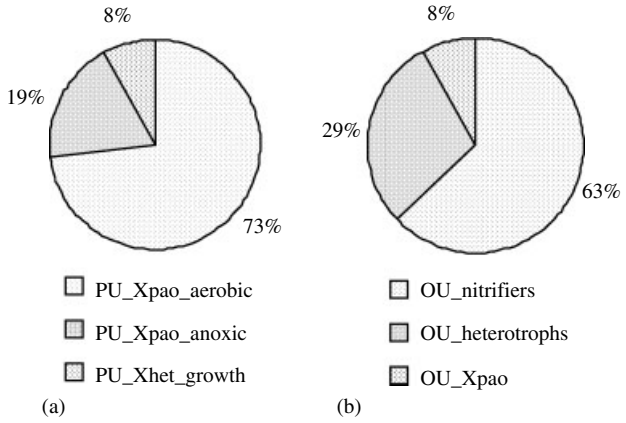

Figure 8. Simulated (a) phosphate utilization and (b) oxygen utilization in one SBR cycle.

the settling phase. The simulations showed that 22 mg L^{-1} NO_3-N was denitrified in one cycle, which is consistent with the denitrification potential calculated according to Ref. 5, which led to a value of 18 mgN L^{-1}. The difference can be explained as follows. First, it should be acknowledged that the 18 mg L^{-1} does not consider the denitrification potential used by the PAOs. Another explanation is the additional denitrification in the aerobic phase due to the low oxygen levels. This is not considered in the stoichiometric calculation. The nitrate utilization rate (NUR) is mainly governed by ordinary heterotrophic activity, i.e. 89% of the total denitrified nitrogen is used up by these microorganisms. The remaining 11% nitrate removal is brought about by denitrifying PAOs [Fig. 7(b)].

The maximum total oxygen uptake rate (OUR) is around 82 mgO_2 L^{-1} h^{-1} until 150 min (nitrification end-point) and is governed by the oxygen transfer capacity [Fig. 7(b)]. During the aerobic phase, the maximum oxygen uptake rates for the autotrophs, heterotrophs and PAOs are around 50, 50 and 10 mgO_2 L^{-1} h^{-1}, respectively. However, these maximum rates are reached in different periods of the aerobic phase (see Fig. 7). The distribution of oxygen consumptions between the processes is given in Fig. 8(b). The autotrophic biomass accounts for 63% of the total oxygen consumption of the system. The ordinary heterotrophs consume only 29%.

CONCLUSION

A systematic model calibration methodology was successfully applied to a laboratory-scale SBR exhibiting simultaneous nitrification–denitrification together with biological phosphorus removal, the so-called 'simultaneous nutrient removal'. The biological processes described in the model were found to occur simultaneously under limited aeration conditions. A low oxygen transfer inherently differentiates the system behavior from systems using traditional design calculations. As a result, the oxygen transfer should strictly be incorporated in the calibration of biological nutrient removal to visualize the individual contributions of each biological process. From this point of view, models serve as practical tools to evaluate alternatives for the optimization of SBRs. The stepwise calibration methodology applied here is necessary for an effective estimation of the relevant parameters.

The systems analysis performed with the calibrated model clearly illustrated that the denitrification at the start of the aerobic phase and during the settling phase makes a considerable contribution to the overall denitrification capacity of the system and also affects enhanced biological phosphate removal. The calibrated models can effectively be used in optimizing the process performance (nutrient removal) together with minimization of operational costs by cycle adjustments, aeration optimization, etc.

ACKNOWLEDGEMENTS

This research was financially supported by the Fund for Scientific Research—Flanders (FWO) and the Ghent University Research Fund.

REFERENCES

1 Artan N and Orhon D, *Mechanism and design of sequencing batch reactors for nutrient removal*, IWA Scientific and Technical Report No: 19, IWA Publishing, London, UK (2005).
2 Irvine RL, Wilderer PA and Flemming HC, Controlled unsteady state processes and technologies, an overview. *Water Sci Technol* **35**(1):11–18 (1997).
3 Ketchum LH Jr, Design and physical features of sequencing batch reactors. *Water Sci Technol* **35**(1):1–10 (1997).
4 Wilderer P, Irvine RL and Goronszy MC, *Sequencing Batch Reactor Technology*, IWA Scientific and Technical Report No: 10, IWA Publishing, London, UK (2001).
5 Artan N, Wilderer P, Orhon D, Morgenroth E and Özgür N, The mechanism and design of sequencing batch reactor systems for nutrient removal—the state of the art. *Water Sci Technol* **43**(3):53–60 (2001).
6 Teichgräber B, Schreff D, Ekkerlein C and Wilderer PA, SBR technology in Germany—an overview. *Water Sci Technol* **43**(3):323–330 (2001).
7 Daigger GT and Littleton HX, Characterization of simultaneous nutrient removal in staged, closed-loop bioreactors. *Water Environ Res* **72**(3):330–339 (2000).
8 Demuynck C, Vanrolleghem P, Mingneau C, Liessens J and Verstraete W, NDBEPR process optimisation in SBRs: reduction of external carbon source and oxygen supply. *Water Sci Technol* **30**(4):169–179 (1994).
9 Hvala N, Zec M, Ros M and Strmcnik S, Design of a sequencing batch reactor sequence with an input load partition in a simulation-based experimental environment. *Water Environ Res* **73**(2):146–153 (2001).
10 Sin G, Insel G, Lee DS and Vanrolleghem PA, Optimal but robust N and P removal in SBRs: a model based study of operation scenarios. *Water Sci Technol* **50**(10):97–105 (2004).
11 Murat S, Insel G, Artan N and Orhon D, Effect of temperature on the nitrogen removal performance of a sequencing batch reactor treating tannery wastewater. *Water Sci Technol* **48**(11–12): 319–326 (2004).
12 Sin G, Van Hulle SWH, De Pauw DJW, van Griensven A and Vanrolleghem PA, A critical comparison of systematic calibration protocols for activated sludge models: a SWOT analysis. *Water Res* **39**:2459–2474 (2005).

13 Shuler ML and Kargi F, *Bioprocess Engineering*, Prentice-Hall, New Jersey, USA (1992).
14 APHA, *Standard Methods for the Examination of Water and Wastewater*, 20th ed. American Public Health Association, Washington DC, USA (1998).
15 Henze M, Gujer W, Mino T, Matsuo T, Wentzel MC, Marais GvR and van Loosdrecht MCM, Activated sludge model No. 2d, ASM2d. *Water Sci Technol* **39**(1):165–182 (1999).
16 Boeije G, Corstanje R, Rottiers A and Schowanek D, Adaptation of the CAS test system and synthetic sewage for biological nutrient removal. Part I: development of a new synthetic sewage. *Chemosphere* **38**(4):699–709 (1999).
17 Orhon D, Okutman D and Insel G, Characterization and biodegradation of settleable organic matter for domestic wastewater. *Water SA* **28**(3):299–305 (2002).
18 Kazmi AA, Fujita M and Furumai H, Modeling effect of remaining nitrate on phosphorus removal in SBR. *Water Sci Technol* **43**(3):175–182 (2001).
19 Vanhooren H, Meirlaen J, Amerlinck Y, Claeys F, Vangheluwe H and Vanrolleghem PA, WEST: modeling biological wastewater treatment. *J Hydroinformatics* **5**:27–50 (2003).
20 Spagni A, Buday J, Ratini P and Bortone G, Experimental considerations on monitoring ORP, pH, conductivity and dissolved oxygen in nitrogen and phosphorus biological removal processes. *Water Sci Technol* **43**(11):197–204 (2001).
21 Comeau Y, Hall KJ and Oldham K, Indirect phosphate quantification in activated sludge. *Water Pollut Res J Can* **25**(2):161–174 (1990).
22 Kuba T, Wachtmeiser A, van Loosdrecht MCM and Heijnen JJ, Effect of nitrate on phosphorus release in biological phosphorus removal systems. *Water Sci Technol* **30**(6):263–269 (1994).
23 Maurer M and Gujer W, Monitoring of microbial phosphorus release in batch experiments using electric conductivity. *Water Res* **29**(11):2613–2617 (1995).
24 Henze M, Grady CPL Jr, Gujer W, Marais GvR and Matsuo T, *Activated Sludge Model No. 1*. IAWPRC Scientific and Technical Report No. 1, IAWPRC Publishing, London, UK (1987).
25 Muller A, Wentzel MC, Loewenthal RE and Ekama GA, Heterotrophic anoxic yield in anoxic aerobic activated sludge systems treating municipal wastewater. *Water Res* **37**(10):2435–2441 (2003).
26 Orhon D, Sözen S and Artan N, The effect of heterotrophic yield on the assessment of the correction factor for anoxic growth. *Water Sci Technol* **34**(5–6): 67–74 (1996).
27 Gujer W and Larsen TA, The implementation of biokinetics and conservation principles in ASIM. *Water Sci Technol* **31**(2):257–266 (1995).
28 Brdjanovic D, van Loosdrecht MCM, Hooijmans CM, Mino T, Alaerts GJ and Heijnen JJ, Innovative methods for sludge characterization in biological phosphorus removal systems. *Water Sci Technol* **39**(6):37–43 (1999).
29 Insel G, Artan N and Orhon D, Effect of aeration on nutrient removal performance of oxidation ditch systems. *Environ Eng Sci* **22**(6):802–815 (2005).
30 Munch EV, Lant P and Keller J, Simultaneous nitrification and denitrification in bench-scale sequencing batch reactors. *Water Res* **30**(2):277–284 (1996).